J Polym Res (2013) 20:245
DOI 10.1007/s10965-013-0245-y

ORIGINAL PAPER

Synthesis and thermal properties of novel room temperature vulcanized (RTV) silicone rubber containing POSS units in polysioxane main chains

Yunhui Shi · Guangsu Huang · Yufeng Liu · Yanbing Qu · Dian Zhang · Yu Dang

Received: 7 May 2013 / Accepted: 13 August 2013 / Published online: 25 August 2013

Abstract Ethyoxyl-phenyl polyhedral oligomeric silsesquioxane (DOPO) was synthesized at first and then copolymerized with polydimethylsiloxane (PDMS) and finally cured to prepare room temperature vulcanized (RTV) silicone rubber (b-POS-SiR). Their structures and properties are characterized and evaluated by fourier transform infrared spectroscopy (FT-IR), nuclear magnetic resonance (NMR), wide angle X-Ray diffraction (WAXD), and dynamic mechanical analysis (DMA). The thermal degradation mechanisms are investigated via thermal gravimetric analysis (TGA) coupled with FTIR analyses. The results show, that the thermal degradation temperatures (5 mass % loss) of the b-POS-SiR are significantly improved with addition of DOPO, e.g., 60 °C and 20 °C higher in nitrogen and in air, respectively, for the b-POS-SiR with 5 wt% DOPO compared that of PDMS rubber (PSiR). The variety of degradation mechanisms in the different atmospheres are also studied by using TGA coupled with FTIR.

Keywords Ethyoxyl-phenyl POSS · RTV silicone rubber · Synthesis · TGA coupled with FTIR · Thermal degradation stability

Introduction

Polyhedral oligomeric silsesquioxane (POSS) has been increasingly used as organic–inorganic hybrid reinforcing nano-filler [1, 2], the rigid building blocks of which are composed of a silicon–oxygen framework and organic substituent groups at corners. The hydrocarbon periphery surrounding the Si-O core can be reactive or chemically inert, hence POSS derivatives can be easily incorporated into polymeric systems via chemical bonds or physical blending to improve their thermal stability [3, 4], mechanical properties [5, 6], and its resistance to environmental degradation [7], ect. However, incorporation of POSS into polymer by simple physical blending would lead to a tendency towards aggregate for higher concentrations due to the weak interreaction between POSS and polymers. Therefore, POSS is covalently bonded to the polymer in most cases. Recently, a variety of such POSS-based polymers has been reported for different systems [8–15].

Polysiloxane is currently under rapid development, which has been widely applied to promote the low carbon economy. As a very promising material, polysiloxane has some unique properties such as low combustion heat, low gas transition temperature, excenllent thermal stability and low chemical reactivity. It is also worth mentioning that polysiloxane is derived from non-petrochemical route and is rich in resources. However, it cannot take the place of carbon based polymers unless certain issues get resolved, such as its poor mechanical properties, insufficient heat-resistant temperature and fire resistance. Incorporating POSS species containing reactive groups into polysiloxane is an attractive project. Compared to the incorporation of POSS by physical blending [16–20], chemical bonding creates the possibility to covalently bond the nanostructured moiety to the polysiloxane chain. To date, several such researches of polysiloxane/POSS nanocomposites have been reported in the literature including; work by Baumann [21] who used POSS as both an cross-linker and nanometric filler in polysiloxane systems to design new elastomeric materials with enhanced mechanical properties. Pan [22] also reported mechanical properties of the enhancing material prepared by chemical attachment of POSS molecules as pendant groups to the polysiloxane chains. These materials

Y. Shi · G. Huang (✉) · Y. Liu · Y. Qu · D. Zhang · Y. Dang
College of Polymer Science and Engineering, State Key Laboratory of Polymer Materials Engineering, Sichuan University, Chengdu 610065, China
e-mail: guangsu-huang@hotmail.com

were subsequently chemically bonded into a polysiloxane network and their mechanical properties were been involved mostly. Nevertheless, the reports of preparation, thermal stability and degradation mechanism of polysiloxane/POSS composites are rare.

To improve the miscibility and interaction between the POSS and the matrix, we firstly reported the preparation of ethyoxyl-phenyl POSS (DOPO) and synthesized hybrid oligomers of polydimethylsiloxane/DOPO through chemical copolymerization and finally obtained a novel room temperature vulcanized (RTV) silicone rubber (b-POS-SiR). In this paper, we investigated the process of copolymerization and the synthesis of POSS modified RTV silicone rubber. Moreover, the thermal degradation process of the silicone rubbers was also studied via thermal gravimetric analysis (TGA) coupled with FTIR analyses.

Experimental

Materials

Ethyoxyl-phenyl POSS (DOPO) was prepared in our laboratory. HPDMS (107#, 3000±300cs) was supplied by Jiangxi Xinghuo chemical Co., LTD, Jiangxi, and platinum(0)-divinyl tetramethyldisiloxane (Pt (dvs)) was supplied by Aoxin New Material Co., Ltd., Shanghai, China. Dibutyltin dilaurate was provided by Zhuorui New Material Co., Ltd., Shanghai, China. Poly(hydrosiloxane) and methyltris(methylethylketoxime)silane were obtained from Taly Chemical Industrial Co.,Ltd., Chengdu, China. The above raw materials were used as received. Toluene and tetrahydrofuran (THF) were purchased from Chengdu Haihong Chemical. The solvents were of analytical purity and dehydrated according to classic literature procedure.

Synthesis of hydrogen–phenyloctasiloxane tetrasodium silanolate [$Na_4O_{14}Si_8Ph_8$]

Hydrogen–phenyloctasiloxane tetrasodium silanolate [$Na_4O_{14}Si_8Ph_8$] was synthesized by the following method reported by Yoshitaka [23]. A 250-ml three-necked flask equipped with a reflux condenser and a dropping funnel was charged with 120 mL 2-propylalcohol, 0.14 mol deionized water, and 0.42 mol sodium hydroxide, and sealed under dry nitrogen. 0.12 mol phenyltrimethoxysilane was added dropwise from the dropping funnel at room temperature for about 60 min while stirred by means of a magnetic stirrer. Then, the reaction mixture was refluxed in an oil bath for 4 h, and continued to stir at 20 °C for 15 h. The deposited precipitate was separated by a pressure filter equipped with a membrane filter. This precipitate was washed once with 2-propyl alcohol and vacuum dried at 70 °C for 5 h, 14.63 g of product was obtained with a yield of 83.5 %.

Synthesis of Dihydrogen -phenylPOSS(DHPO) [$Ph_8Si_{10}O_{14}H_2Me_2$]

In a typical reaction, 30 mmol triethylamine and 30 mmol methydichlorosilane was injected into a 200 mL single-necked flask with a solution of 10 mmol $Na_4O_{14}Si_8Ph_7$ and anhydrous THF (100 mL) under stirring. Stirring was further continued at room temperature for 1 h, and then water (50 mL) was added to dissolve sodium chloride formed during the reaction and hydrolyze unreacted methyldichlorosilane. The reaction mixture thus obtained was transferred to a separating funnel. The organic fraction was washed with 1 N hydrochloric acid or saturated sodium bicarbonate solution (aqueous) until the pH reached 7, then further washed three times with ion-exchanged water. The organic layer was isolated and dried over $MgSO_4$ for 20 min. Finally, white powder was obtained by removing solvent and volatiles via rotary evaporation at 70 °C, which was further dried in an vacuum oven at 70 °C for 5 h to get a constant weight. 6.82 g pale powder with the yield of 59 % was obtained.

Synthesis of ethyoxyl-phenyl POSS (DOPO) [$Ph_8Si_{10}O_{14}(OCH_3)_2Me_2$]

Ethyoxyl-phenyl POSS (DOPO) [$Ph_8Si_{10}O_{14}$ $(OCH_3)_2Me_2$] was synthesized via the hydrosilylation between $Ph_8Si_{10}O_{14}H_2Me_2$ and ethoxydimethylvinylsilane. The general preparation procedures are as follows, 2.2 g DHPO, 2 g ethoxydimethylvinylsilane, 0.1 mL Pt (dvs) and 50 ml anhydrous THF were charged into a 100 mL single-necked flask equipped with a magnetic stirrer. The flask was sealed with dry nitrogen and heated in an oil bath under stirring, while THF was refluxed. Then the reaction mixture was allowed to react for 33 h to access a complete reaction. The reaction mixture was concentrated with rotary evaporation to obtain 1.03 g of brown powdery solid matter. The product DOPO was used in the following experiments without further purification. $Ph_8Si_{10}O_{14}(OCH_3)_2Me_2$ ^{29}Si NMR (solvent:$CDCl_3$): δ(ppm), −78.59 (s, 4Si), −78.06 (s,3Si), −79.55 (s,4Si), −16.05 (s,1Si), 18.0 5 (s,1Si). FTIR (cm^{-1}, KBr window): 1200–950 cm^{-1} (Si-O-Si), 1430, 1590 cm^{-1} (Si-Ph), 940 cm^{-1} (Si-O-C).

Synthesis of poly(dimethylsiloxane)s with POSS in the polysiloxane main chain (DOPO-PDMS)

DOPO-PDMS was prepared according to the procedures described in Scheme 1, We have prepared a series of DOPO-PDMS copolymers for thermal properties investigations. And typical experimental procedures are given as follows.

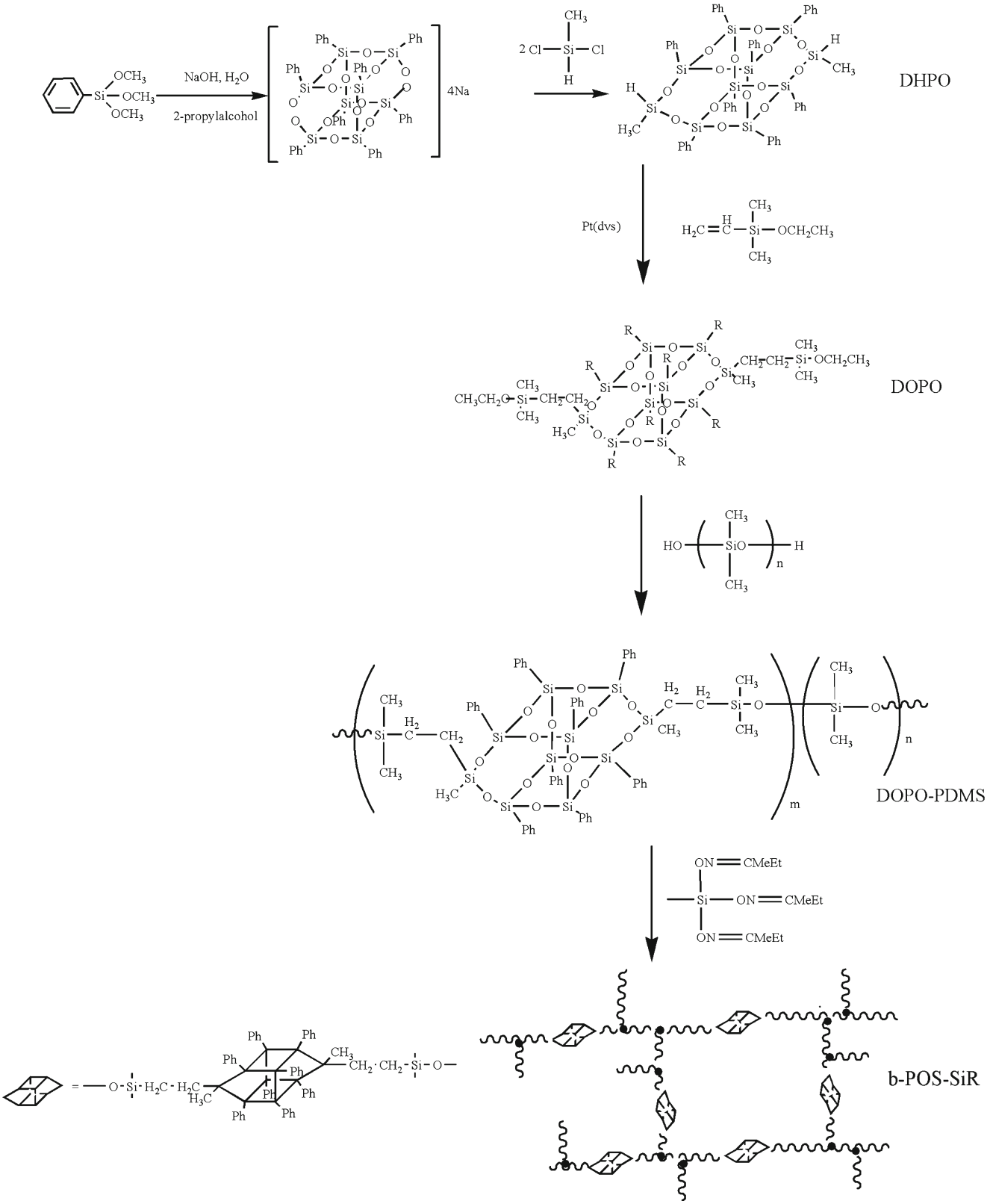

Scheme 1 Synthetic routes for DOPO and RTV silicon rubber with POSS in the main chain

In a typical reaction, 1.6 g DOPO and 30 g PDMS were dissolved in 80 mL toluene via agitation in a 250 mL three-necked flask with a magnetic stirrer, then 0.15 g dibutyltin dilaurate was added. The reaction mixture was stirred at 100 °C

for 1 h to access a complete reaction. The reaction mixture was concentrated with rotary evaporation and a 30.4 g yield was obtained through this procedure.

Preparation of the silicon rubber containing POSS in the main chain (b-POS-SiR)

The preparation procedures of room temperature vulcanized silicone rubber is as follows (Scheme 1). DOPO-PDMS polymer, methyltris(methylethylketoxime)silane and dibutyltin dilaurate were charged into a three-necked flask under dry nitrogen and stirred by mechanical stirrer. The reaction mixture was obtained after stirring for 15 min. The mixture was then poured into a Teflon mould subsequently, and cured for about 2 day at room temperature to get a sheet of RTV silicone rubber with smooth surface.

As reference material, we also synthesized RTV silicone rubbers using HPDMS polymer named PSiR according to the same approach above.

Measurement and techniques

^{1}H NMR and ^{29}Si NMR spectra were recorded on a Bruker AV 11–400 spectrometer at 600 and 400 MHz in $CDCl_3$ (0.05%TMS as an internal standard) at RT, respectively. FTIR spectra were measured with a spectral resolution of 2 cm^{-1} on a Nicolet Magna 560 infrared analyzer using KBr disks or pellets at room temperature. Wide Angle X-Ray Diffraction (WAXD) was used to investigate the distribution of POSS in the silicone rubber. The WAXD measurements were conducted with a Philips X' Pert Graphics & Identify. To investigate the viscous-elastic characteristic of samples, dynamic mechanical analysis (DMA; temperature scan at 1 Hz and 1 % strain) was carried out at a constant rise of temperature (2 °C•min^{-1}) from −130 °C to ambient temperature. Thermo gravimetric analysis (TGA) coupled with FTIR were carried out using a Perkin-Elmer and Nicolet Magna 560. About 10 mg of sample cut into small pieces was loaded in alumina pans in nitrogen and in air atmosphere from ambient temperature to 800 °C at a constant rise of temperature (10 °C•min^{-1}).

Results and discussion

Characterization of the RTV silicon rubber containing POSS in the main chain (b-POS-SiR)

In this study, DHPO and DOPO were firstly prepared. Figure 1 shows the FTIR spectra of DHPO and DOPO in the regions from 4000 to 500 cm^{-1} where the Si–O–Si absorption bands in both samples are displayed in the range of 1300–950 cm^{-1}. The FTIR data reveals that the DHPO has the

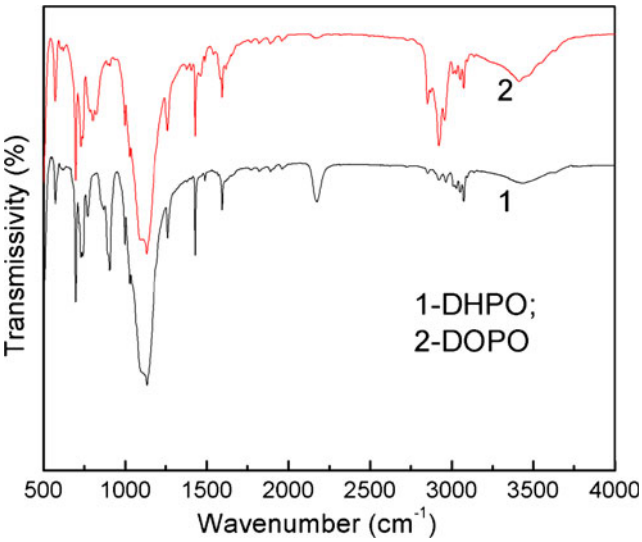

Fig. 1 FTIR spectra of DHPO and DOPO

Si-H characteristic peak at 2173 cm^{-1}, and this characteristic peak disappears in the FTIR spectra of the DOPO, because the Si-H group reacts with ethoxydimethylvinylsilane via the hydrosilylation and the absorption band is replaced by Si-O-C at 940 cm^{-1}.

The successful synthesis of the silicon rubber containing POSS in the main chain (b-POS-SiR) was confirmed by its FTIR spectrum. As displayed in Fig. 2, the Si-O-C stretching vibration peak in DOPO at 940 cm^{-1} is disappeared in copolymer, while other characteristic bands of the DOPO appears after condensation, including the asymmetric stretching vibration of Si–O–Si at 1300–950 cm^{-1} and the stretching vibration of -C-H- for Si-CH_2-CH at 2917 cm^{-1} and 2848 cm^{-1}. These results imply that DOPO has reacted with PDMS and vulcanized to form b-POS-SiR rubber.

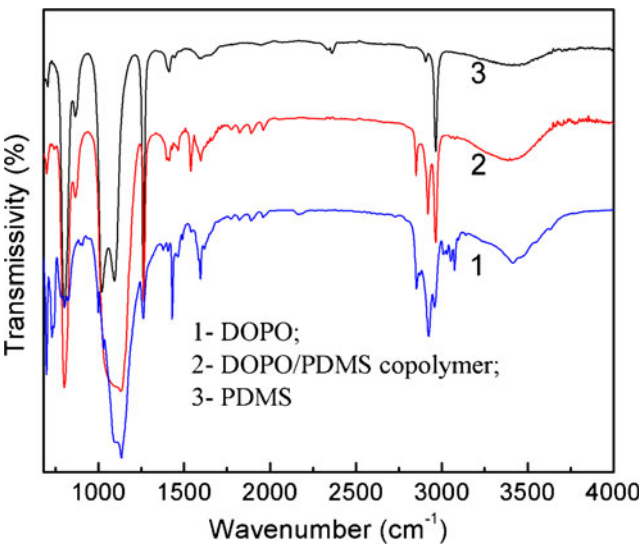

Fig. 2 FTIR spectra of DOPO and PSiR after reaction

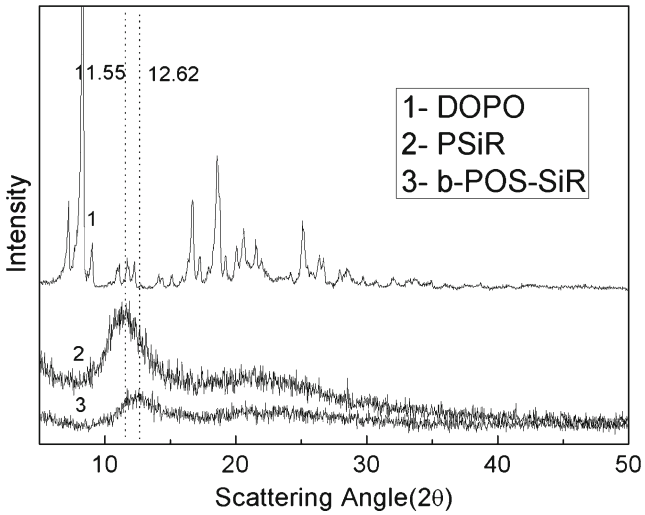

Fig. 3 WAXD patterns of PSiR, DOPO and b-POS-SiR

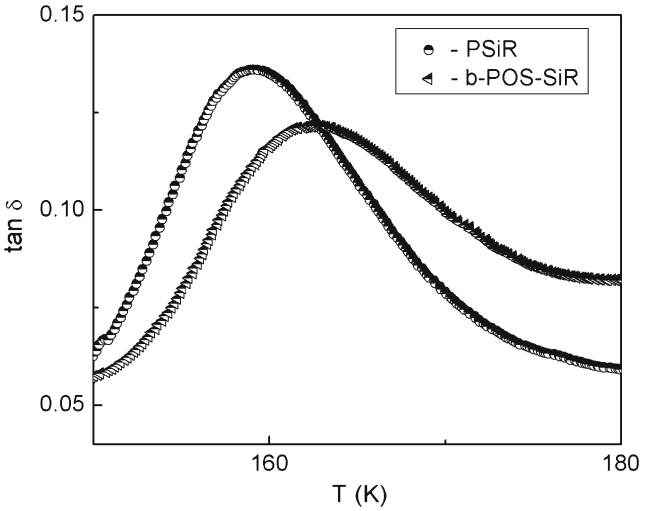

Fig. 5 Tanδ curves for PSiR and b-POS-SiR

To observe and evaluate the dispersion uniformity of POSS, WAXD measurements were performed. Figure 3 displays the resulting X-ray diffraction curves from crosslinked PDMS rubber (PSiR) and b-POS-SiR Nanocomposites. The WAXD pattern of DOPO reveals intense and sharp crystalline reflections at the entire scanning range, indicating a high degree of crystallinity and an ordered structure of DOPO. Unlike DOPO, diffuse amorphous reflections appears in PSiR approximately at 2θ=11.55° and 2θ=22° and no crystalline peaks of PSiR are detected at room temperature condition. Copolymerization of polysiloxane with DOPO leads to the amorphous reflections that appears from 11.55° to 12.62°, which enhanced the rigidity of b-POS-SiR molecular chains and formed a portion-range ordered structure just like Liquid-crystal structure in main chain. The framework distance decreases appreciably as the average interchain distance deceases along with X-ray diffraction results. In addition, the WAXD data give no indication of the presence aggregate of DOPO crystalline in the synthesized nanocomposites.

DMA measurement was peformed for b-POS-SiR and PSiR, the resulting loss modulus E″ and tan δ curves are shown in Figs. 4 and 5, respectively.

The temperature corresponding to the α relaxation as the loss modulus E″ characterized in Fig. 4 is observed to increase approximately 3.14 K for b-POS-SiR over pure PSiR. The tan δ curves of pure PSiR, on the other hand, as shown in Fig. 5 indicates that the glass transition temperature (Tg) is at 159.03 K, while the Tg of the b-POS-SiR rubber is slightly increased (3.66 K) compared to that of the pure PSiR as the maximal peak represents the α transition to a higher temperature. And in addition, the tanδ peak broadens significantly. Such peak broadening reveals that polymerizing with POSS is necessary to partially affect the polymer chain mobility. These observations suggest a faint nanoreinforcement effect

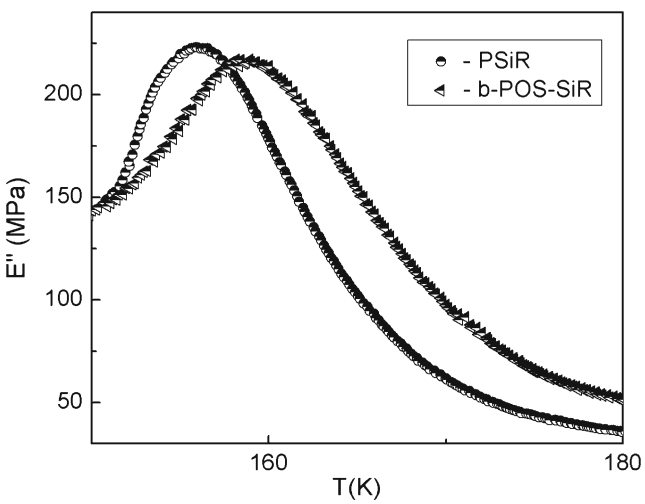

Fig. 4 Loss modulus E″ curves for PSiR and b-POS-SiR

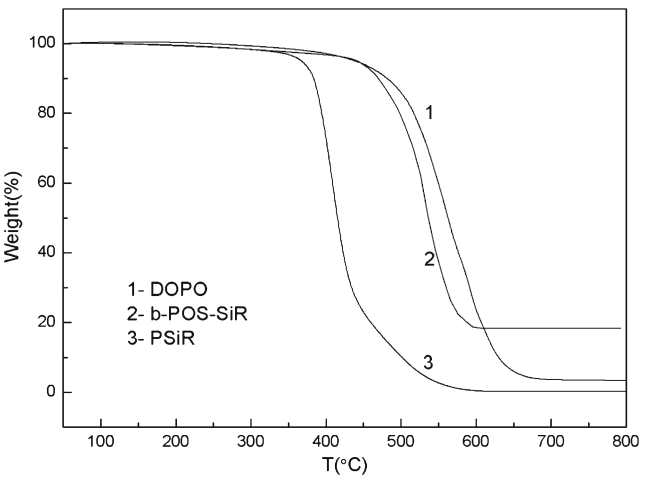

Fig. 6 TGA thermograms of DOPO, PSiR and b-POS-SiR obtained in nitrogen atmosphere

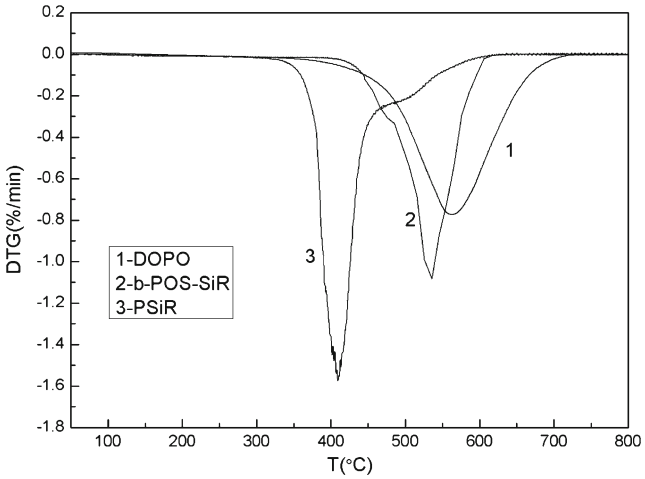

Fig. 7 DTG curves for DOPO, PSiR and b-POS-SiR obtained in nitrogen atmosphere

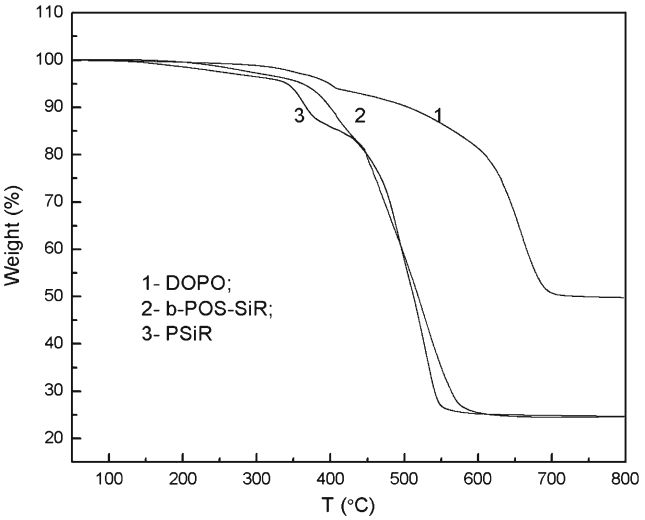

Fig. 8 TGA thermograms of DOPO, PSiR b-POS-SiR obtained in air atmosphere

generated from the rigid bulky POSS cages and an increase in Tg may originate from POSS which restricts the molecular rotation motions and reduce the conformational numbers of macromolecular chains, thus higher temperature is required to overcome the raise of activation energy of chain segmental motion caused by POSS.

Thermal degradation stability

Figures 6 and 7 show the TGA and DTG curves of pure DOPO, PSiR and b-POS-SiR with 5 wt% DOPO in nitrogen atmosphere at a heating rate of 10 °C/min. Other important features of the thermograms for all three samples are shown in Table 1.

As shown in Fig. 6 (TGA), the temperatures of 5 % mass loss of pure DOPO and PSiR are 400 °C and 340 °C, respectively. The b-POS-SiR copolymer, with a 5 wt% content of DOPO, exhibits good thermal stability up to 400 °C, and the residue yield ranging from 0.18 % to 18.26 % are observed at 800 °C in nitrogen atmosphere. As can be seen from Fig. 7 (DTG), the temperatures of maximum weight loss of DOPO and PSiR are 563 °C and 409 °C, respectively. For b-POS-SiR, the temperature of maximum weight loss is 536 °C, which is 127 °C higher than that of PSiR and only 27 °C lower compared with DOPO. The results mentioned above demonstrate, that POSS plays a significant role in enhancing the thermal stability of the b-POS-SiR. Besides, there are two characteristic temperatures of degradation peak appearing at higher temperature for b-POS-SiR and PSiR, which probably suggests the existence of different degradation mechanisms, as discussed latter in the following section.

Table 1 Thermal properties of PSiR and b-POS-SiR obtained in nitrogen

	PSiR	b-POS-SiR
POSS wt%	0	5
The temperature of 5 % weight loss (°C)	340	400
The temperature of the greatest amount of weight loss (°C)	409	536
The degradation residual yields (%)	0.18	18.26

The thermo-oxidative behavior in air is obviously more complex than the degradation behavior in nitrogen atmosphere. As demonstrated in Fig. 8 (TGA) and Fig. 9 (DTG), the temperatures of 5 % mass loss of pure DOPO and PSiR are 398 °C and 341 °C, respectively. For b-POS-SiR, when the content of DOPO was 5 wt%, the temperature of 5 % mass los is delayed to 362 °C, which is 21 °C higher than that of PSiR and 36 °C lower compared with DOPO. However, its thermo-oxidative residue at 800 °C is almost the same as PSiR. Other important features of the thermograms for all three samples under air are given in Table 2. Two obvious degradation steps are observed for all the samples, which probably involve a

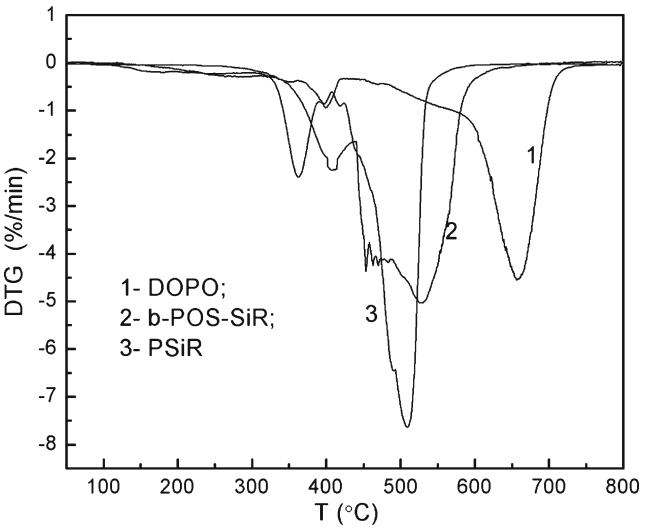

Fig. 9 DTG curves for PSiR and b-POS-SiR obtained in air atmosphere

Table 2 Thermal properties of PSiR and b-POS-SiR obtained in air

	PSiR	b-POS-SiR
POSS wt%	0	5
The temperature of 5 % weight loss (°C)	341	362
The temperature of the greatest amount of weight loss (°C)	562	599
The degradation residual yields (%)	24.66	24.60

complex competition between crosslinking [24] and degradation, different from the mechanisms in N_2. The different degradation mechanisms in N_2 and air would be discussed in the following section.

Degradation mechanism

From the discussions above, copolymerizing with POSS is indeed beneficial to improve the thermal degradation stability of PSiR. In order to clarify the mechanism, measurements of thermal gravimetric coupled with IR were performed.

Based on our previous work, there is only a hump from 441 °C to 470 °C but a major weight loss appeared from 481 °C to 609 °C in the DTG curves for b-POS-SiR (polymethylsiloxane) in nitrogen atmosphere. Thermal gravimetric analysis (TGA) coupled with FTIR was used to analyze the gas products of thermal degradation. Figure 10 shows the FTIR spectra at different temperatures. Obvious peaks are observed at 2970, 1265, 1095, 1026, 814 cm^{-1} from 441 °C to 470 °C, indicating that some tiny cyclized D_3 and D_4 generated, and the relative concentration of D_3 and D_4 keep increasing slightly. Similarly, the concentration of D_3, D_4 and dimethyl siloxane increase distinctly as the intensity of peaks at 2970, 1265, 1095, 1026 and 814 cm^{-1} increase obviously from 481 °C to 609 °C. How could this degradation progress happen?

Essentially, it is well-known that different degradation mechanisms occurred for different PSiR. Mainly four different mechanisms have been proposed for thermal degradation of PSiR in inert atmosphere due to variations in the method of preparation, the level of impurities and residual catalyst, and the degradation of conditions [24]. The four mechanisms include, (a) the end-initiated unzipping mechanism [25–28]; (b) the random main chain scission mechanism [27]; (c) the externally catalyzed mechanism for polymers containing

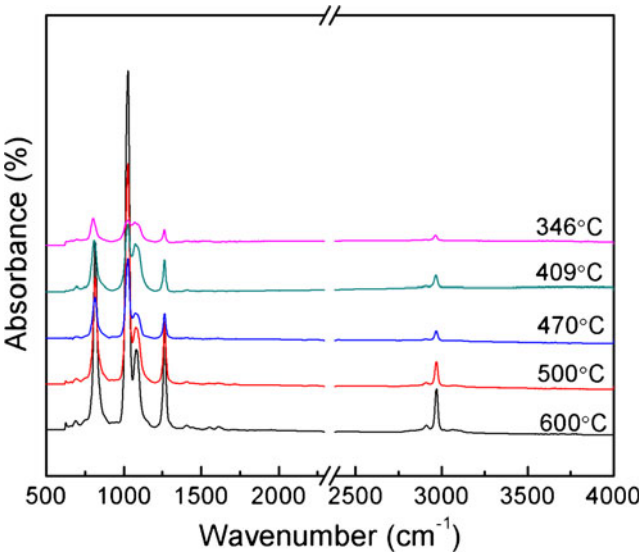

Fig. 11 FTIR spectra of thermal degradation products for PSiR sample at different temperature in nitrogen

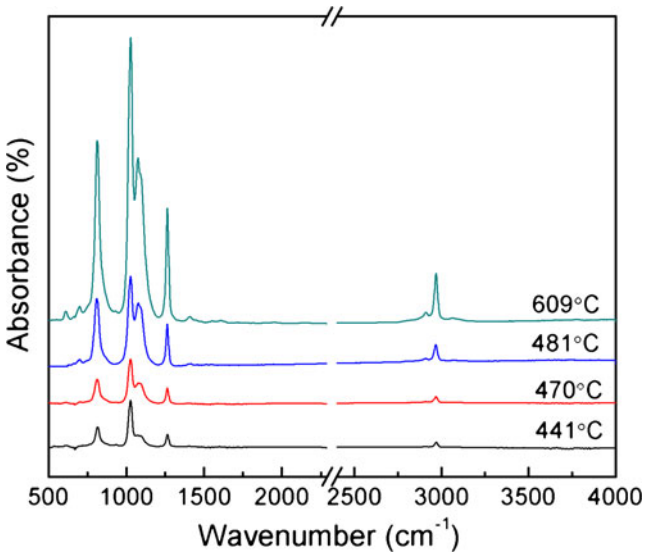

Fig. 10 FTIR spectra of thermal degradation products for b-POS-SiR sample at different temperature in nitrogen

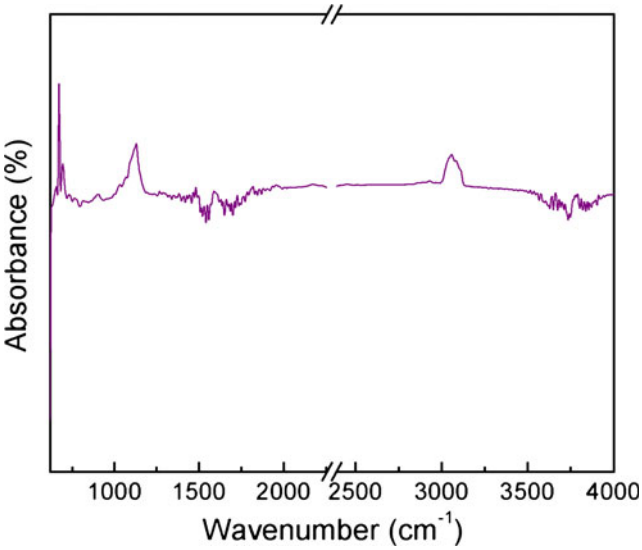

Fig. 12 FTIR spectra of product for DOPO at 547 °C in nitrogen

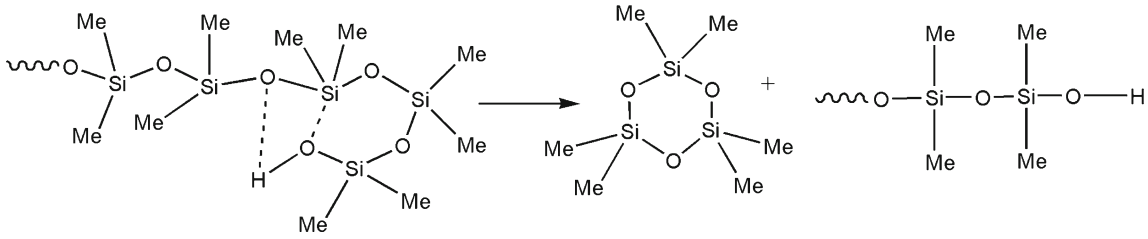

Scheme 2 Thermal degradation mechanism of b-POS-SiR /PSiR

impurities and residual catalyst [29]; and (d) molecular mechanism [27, 28, 30]. Consequently, it would be an interesting challenge to figure out the following questions: Which mechanism is the dominative one for b-POS-SiR degradation? Does POSS cause a change in the degradation mechanism of b-POS-SiR?

Figure 11 shows the FTIR spectra resulting from the gas of PSiR thermal decomposition in nitrogen. A number of peaks can be observed at 2907, 1262, 1082, 1018 and 814 cm^{-1} from 346 °C to 470 °C, indicating that some tiny cyclized D_3 and D_4 generated. Moreover, the intensity of absorption peaks at 2907 and 1262 cm^{-1} are almost changeless from 346 °C to 470 °C suggesting that the relative concentration of D_3 and D_4 are approximately identical. The release of cyclic oligomers is due to the incomplete reacted terminal OH of PSiR which can participate in a 'back biting' reaction in accordance with the end-initiated unzipping mechanism, displaying that the Si-O bond scission takes place from the chain ends and annulations forming in the presence of Si-OH is much easier than that of polysiloxane without Si-OH. The decreases absorption at 1082 cm^{-1} and increases absorption at 1018 cm^{-1} indicates that cyclized D_5 and D_6 are generated when the temperature elevated to 500~600 °C. On the other hand, the intensity of peaks at 2907 and 814 cm^{-1} increase obviously, demonstrating a rise in the concentration of D_3 and D_4. That is due to the thermal depolymerization of the basic chains of the PSiR polymers.

In order to clarify the effect of POSS when it is introduced into PSiR, we also studied the thermal degradation behavior of DOPO.

As displayed in Fig. 12, because of the inert inorganic caged framework of Si-O-Si, DOPO displays striking thermal stability. The spectra of the gas products in nitrogen are definitely the same with DOPO, which is owe to the sublimation of DOPO. In other words, DOPO shows outstanding thermal stability that is still not decomposed but sublimated under the testing condition.

Contrast to PSiR and DOPO, during the degradation process of b-POS-SiR, some tiny cyclized D_3 and D_4 generate and keep increasing slightly from 441 °C to 470 °C, showing the same phenomenon as PSiR degradation. In this case, we propose that the release of cyclic oligomers is due to the incomplete reacted terminal OH in b-POS-SiR that could participate in the 'back biting' reaction in accordance with the end-initiated unzipping mechanism, just the same as PSiR [24, 27, 31]. And the temperature moves to a higher region

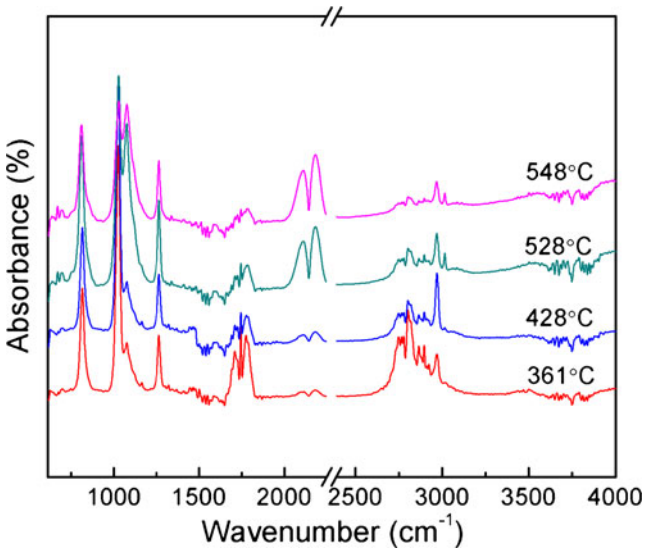

Fig. 13 FTIR spectra of thermal degradation products for b-POS-SiR sample at different temperature in air

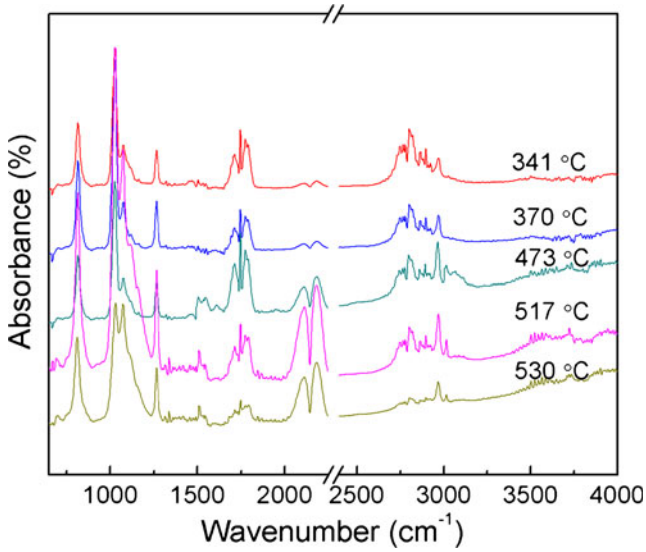

Fig. 14 FTIR spectra of thermal degradation products for PSiR sample at different temperature in air

Scheme 3 Random degradation of PSiR

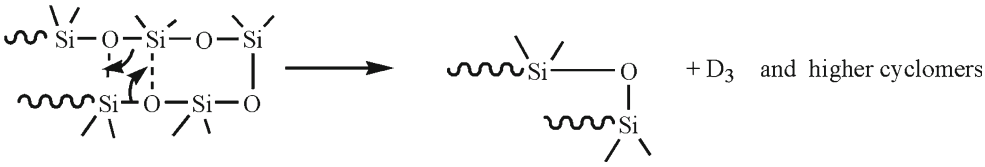

resulting from two main reasons: (a) copolymerizing with DOPO would consume part of OH in PSiR which meant the probability of 'back biting' reaction would go down; (b) incorporating the rigid bulky DOPO cages into the molecular main chain might restrict the molecular mobility and exert nanoreinforcement effect on macromolecular chains (which is confirmed by Tg measured with DMA as indicated above). The likely cyclization reaction mechanism involving OH groups is illustrated in Scheme 2.

On the other hand, the second degradation step of b-POS-SiR is expressed as the concentration of D_3, D_4 and dimethyl siloxane increase distinctly from 481 °C to 609 °C. That is due to the breakage of b-POS-SiR main chain which is caused by increasing chain mobility as the temperature is elevated.

Thermo-oxidative degradation mechanism

The FTIR spectra of b-POS-PSiR and its gas products of thermal degradation at different temperatures in air are shown in Fig. 13. Peaks at 2970, 1265, 1095, 1026, 814 cm^{-1} are first observed as the degradation started. And the major degradation products are a similar mixture of oligomers as in nitrogen with additional CO_2 and H_2O. However, there are two characteristic degradation peaks which showed reflections for both DOPO and PSiR in Fig. 9 (DTG). The temperatures of the two degradation states are delayed and compared with PSiR under air.

The degradation patterns of PSiR in air are much different from that in nitrogen. The IR spectra of PSiR and its gas products of thermal degradation at different temperatures are shown in Fig. 14. In air there are at least two stages of degradation. At the first stage from 341 °C to 368 °C, peaks are observed at 2907, 1265, 1082, 1018 and 841 cm^{-1}, indicating that some tiny cyclized D_3 and D_4 generated at a much lower temperature than that in nitrogen, the reason of which might be oxygen catalyzed decomposition to cyclic oligomers. And the intensity of absorption peak at 2907 cm^{-1} is increased, suggesting that relative concentration of D_3 in the products varied much as the temperature increases, and it may be attributed to some contribution from random degradation (Scheme 3) besides end-initiated degradation.

However, as aforementioned in Fig. 9 (DTG), weight loss of the first degradation step is about 15 %, and subsequently the volatilization slow down. That probably involve a complex competition between crosslinking [24] and degradation, which would be expressed in the below section.

The second degradation stage between 473 °C and 800 °C should be assigned to the thermo-oxidative process of the methyl side groups. The intensity of peak at 3016 cm^{-1} is attributed to methane. The production of methane indicate that random cleavage of Si-CH_3 bonds is involved in addition to the thermal depolymerization of the basic chains of the PSiR polymers (Scheme 4).

In order to clarify the effect of POSS when it is introduced into PSiR, we studied the thermal degradation behavior of DOPO as well.

DOPO displays a different thermal behavior in air and there are also two degradation states to be observed. The first is from 398 °C to 409 °C and the second is from 550 °C to 680 °C. The FTIR spectra of the gas products in air at the first degradation state are definitely the same with DOPO, which is attributed to the sublimation of DOPO.

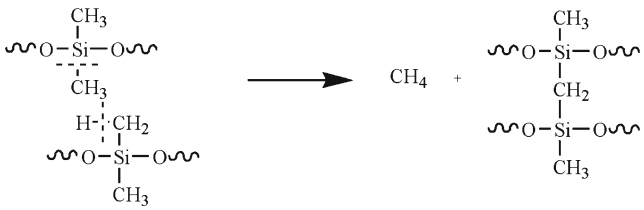

Scheme 4 Crosslinking of b-POS-SiR /PSiR in air

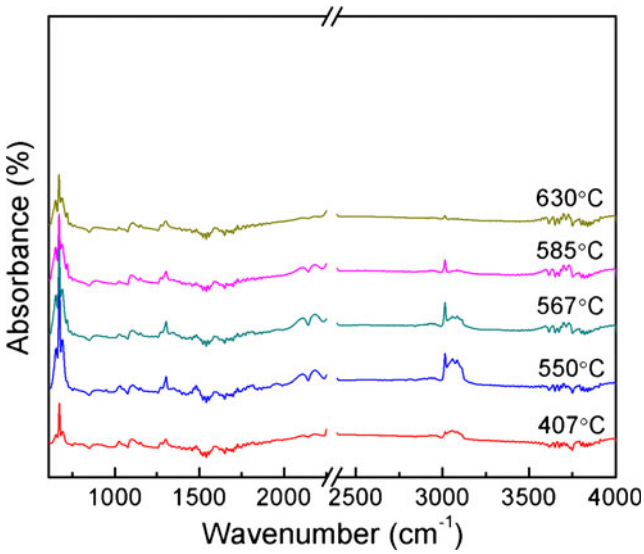

Fig. 15 FTIR spectra of product for DOPO in air

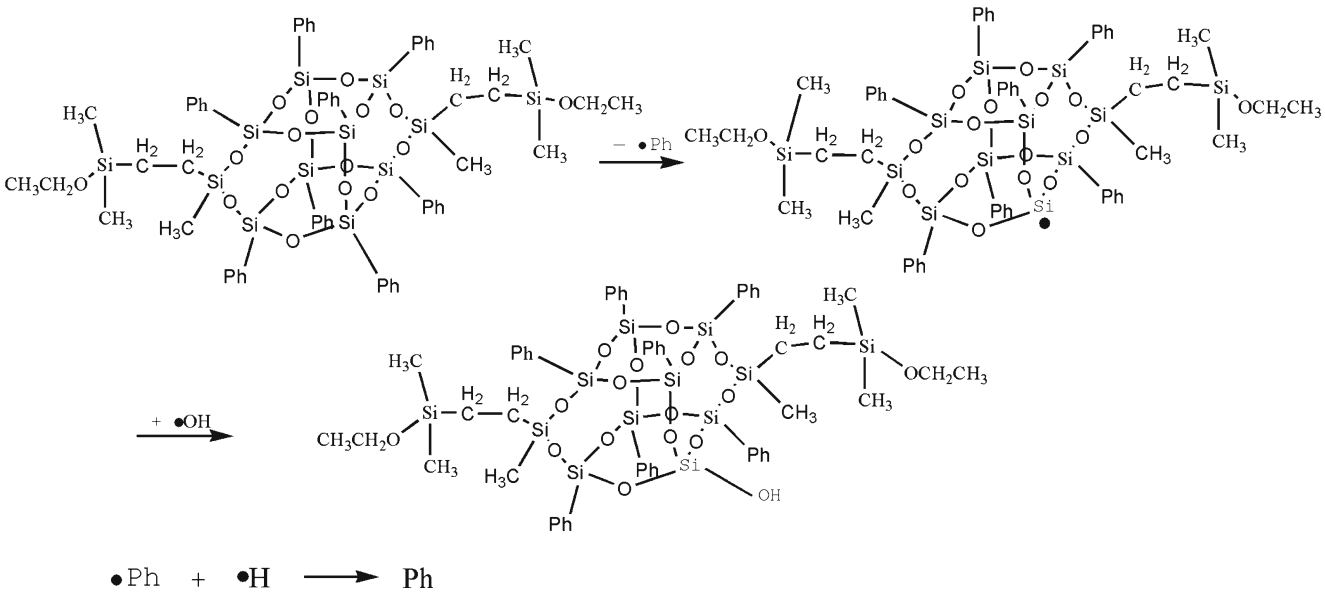

Scheme 5 Thermal degradation mechanism of DOPO between 550 °C and 630 °C in air

A peak appears at 3016 cm^{-1} as temperature elevated to 550 °C, as depicted in Fig. 15, which is attributed to saturated and unsaturated hydrocarbons, especially methane. The absorption peak around 1500 cm^{-1} from 550 °C to 630 °C indicate that benzene series might generate because of the breakage of Si-Ph accompany with the sublimation of DOPO(Scheme 5). The remaining residue is 49.73 %, showing the extrusive thermal stability of DOPO.

Comparatively speaking, the temperatures of the two degradation states for b-POS-SiR are delayed compared with those of PSiR in air. The incorporation of DOPO reduces the flexibility of molecular chain and hinders the random degradation and end-initiated degradation, which would shift the degradation toward a higher temperature. The complex competition between crosslinking [24] and degradation in first degradation stage is expressed as Scheme 6.

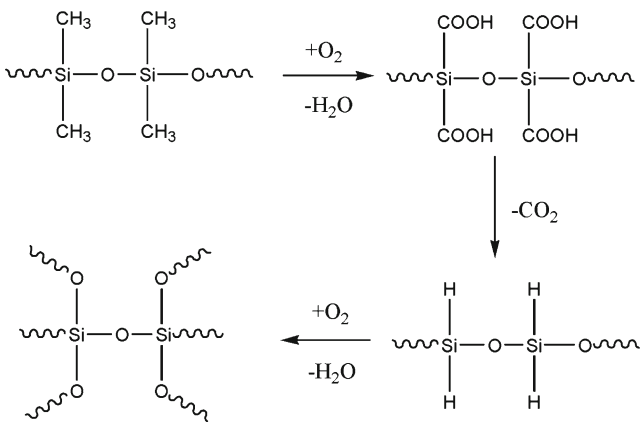

Scheme 6 Thermal degradation mechanism of b-POS-SiR /PSiR in air

As shown in Scheme 6, the major degradation products are a similar mixture of oligomers as in nitrogen with additional CO_2 and H_2O.

The second degradation stage could be explained by the activation energy of Si-C and Si-O bonds [32]. Although the Si-C (318 kJ/mol) bond is thermodynamically less stable than the Si-O (451 kJ/mol) bond, kinetically paths the PSiR rearrangement is not dominant for the required activation energy, which would lead to the production of cyclic oligomers before methane.

However, its thermo-oxidative residue at 800 °C which is almost the same with PSiR reveals that the improvement of thermo-oxidative stability is negligible for b-POS-PSiR.

Conclusion

In summary, POSS is crucial to improve the thermal stabilities of b-POS-SiR. Different degradation mechanisms occurred during different degradation process. The results show that the depolymerization of b-POS-SiR in nitrogen atmosphere is mainly controlled by an end-initiated unzipping mechanism accompanied with a fraction of random degradation mechanism. However, it mainly depolymerizes through random degradation mechanisms, following a radical mechanism in air. Two aspects should be taken into account for this experimental result: (1) a given OH is consumed in the chain extending reaction between DOPO and hydroxy terminated polydimethylsiloxane which would decline the probability of OH terminal initiated unzipping and (2) the tethering of the structure of the POSS cage hinder the cyclization reactions, while the former one is a peculiar degradation reactions in

nitrogen atmosphere and the latter is mainly degradation reactions for both degradation progress.

Acknowledgments The authors acknowledge the support from funding provided by the National Natural Science Foundation of China (Grant No. 51073097).

References

1. Joshi M, Butola BS (2004) J Macromol Sci C Polym Rev 44:389
2. Xu H, Yang B, Wang J, Guang S, Gun L (2007) J Polym Sci A Polym Chem 45:5308
3. Lee L, Chen W (2005) Polymer 46:2163
4. Huang J, He C, Xiao Y, Mya KY, Dai J, Siow YP (2003) Polymer 44:4491
5. Kim GM, Qin H, Fang X, Sun FC, Mather PT (2003) J Polym Sci B Polym Phys 41:3299
6. Jones IK, Zhou YX, Jeelani S, Mabry JM (2008) Express Polym Lett 2:494
7. Wright ME, Petteys BJ, Guenthner AJ, Fallis S, Yandek GR, Tomczak SJ, Minton TK, Brunsvold A (2006) Macromolecules 39:4710
8. Su CH, Chiu YP, Teng CC, Chiang CL (2010) J Polym Res 17:673
9. Lichtenhan JD, Vu NQ, Jason AC, Gilman JW, Feher FJ (1993) Macromolecules 26:2141
10. Ryu HS, Kim DG, Lee JC (2010) Polymer 51:2296
11. Lee A, Lichtenhan JD (1998) Macromolecules 31:4970
12. Fei M, Jin BK, Wang WP, Liu L (2010) J Polym Res 17:19
13. Bizet S, Galy J, Gérard JF (2006) Polymer 47:8219
14. Bharadwaj RK, Berry RJ, Farmer BL (2000) Polymer 41:7209
15. Ohno K, Sugiyama S, Koh K, Tsujii Y, Fukuds T, Yamashio M, Oikawa H, Yamamoto Y, Ootake N, Watanabe K (2004) Macromolecules 37:8517
16. Lichtenhan JD, Otonari YA, Carr MJ (1995) Macromolecules 28:8435
17. Wu J, Haddad TS, Kim GM, Mather PT (2007) Macromolecules 40:544
18. Liu L, Tian M, Zhang W, Zhang L, Mark JE (2007) Polymer 48:3201
19. Liu YR, Huang YD, Liu L (2007) Compos Sci Technol 67:2864
20. Majumdar P, Lee E, Gubbins N, Stafslien SJ, Daniels J, Thorson CJ, Chisholm BJ (2009) Polymer 50:1124
21. Baumann TF, Jones TV, Wilson T, Saab AP, Maxwell RS (2009) J Polym Sci A Polym Chem 47:2589
22. Pan G, Mark JE, Schaefer DW (2003) J Polym Sci B Polym Phys 41:3314
23. Kazuhiro Y, Morimoto Y, Watanabe K, Ootake N (2004) US patent application publication PCT/JP2003/011277
24. Camino G, Lomakin SM, Lazzari M (2001) Polymer 42:2395
25. Lewicki JP, Pate M, Morrel P, Liggat J, Murphy J, Pethrick R (2008) Sci Technol Adv Mater 9:24403
26. Chen D, Yi S, Wu W, Zhong Y, Liao J, Huang C, Shi W (2010) Polymer 51:3867
27. Grassie N, Macfarlane IG (1978) Eur Polym J 14:875
28. Thomas TH, Kendrick TC (1969) J Polym Sci A-2 7:537
29. Grassie N, Macfarlane IG, Francey KF (1979) Eur Polym J 15:415
30. Kucera M, Láníková J, Jelinek M (1961) J Polym Sci 53:301
31. Nikitina TS, Khodzhemirova LK, Aleksandrova YA (1968) Polym Sci 10:1078
32. Camino G, Lomakin SM, Lageard M (2002) Polymer 43:2011